Paper III

Støren, E.N., Kolstad, E.W. and Paasche, Ø. (submitted) Linking past flood frequencies in Norway to regional atmospheric circulation anomalies. *Submitted to Journal of Quaternary Science*

Linking past flood frequencies in Norway to regional atmospheric circulation anomalies

Eivind N. Støren[1,2*], Erik W. Kolstad[2,3] and Øyvind Paasche[2,4]

[1]Department of Earth Science, University of Bergen, Allégt. 41, 5007 Bergen, Norway

[2]Bjerknes Centre for Climate Research, Allégt. 55, 5007 Bergen, Norway

[3]Uni Bjerknes Centre, Allégt. 55, 5007 Bergen, Norway

[4]Now at: Department of Research Management, University of Bergen, Prof. Keysers gate 8, 5020 Bergen, Norway.

*Corresponding author. E-mail address: eivind.storen@geo.uib.no

Bjerknes Centre for Climate Research, Allégt. 55, N-5007, Norway.

Phone/Fax: +47 55589841/+47 55589416.

Abstract:

Analysis of two continuous, high-resolution paleo-flood records from Southern Norway reveals that the frequency of extreme flood events has changed significantly during the Holocene. During the early and middle Holocene, the flood frequency was low; whereas it was high over the last 2300 years when the mean flood frequency was about 2.5 to 3.0 per century. The present regional discharge regime is dominated by spring/summer snowmelt, and our results indicate that the changing flood frequency cannot be explained by local conditions associated with the respective catchments of the two lakes, but rather long-term variations of solid winter precipitation and related snowmelt. Applying available instrumental winter precipitation data and associated sea level pressure re-analysis data as a modern analogue, we document that atmospheric circulation anomalies, significantly different from the North Atlantic Oscillation (NAO), have some potential in explaining the variability of the two different paleo-flood records. Centennial-scale patterns in shifting flood frequency might be indicative of shifts in atmospheric circulation and shed light on paleo-pressure variations in the North Atlantic region, in areas not influenced by the NAO. Major shifts are found at about 2300, 1200 and 200 years ago (cal. a BP).

Keywords: Floods, Atmospheric Circulation, North Atlantic Oscillation, Holocene, Norway

Introduction

A number of Earth System Models (ESM) and Atmosphere–Ocean General Circulation Models (AOGCMs) predict changes in the regional distribution of rainfall due to global warming (e.g., Allen and Ingram, 2002; Solomon *et al.,* 2009), including an increase in the frequency and magnitude of hydrologic extremes, such as floods and droughts, which are expected to impact civilizations across the globe (McCarthy *et al*., 2001; IPCC, 2007). Areas lying north of 60 °N generally show an increase in precipitation, approximately linearly scaled to the temperature increase (Solomon *et al.,* 2009). More precipitation in the North Atlantic sector might lead to an increase in floods, but the connection between changes in the distribution of rainfall and flooding is not straightforward. The main reason for this is that questions concerning precipitation characteristics (the amount of solid precipitation versus rainfall, intensity of rainstorms etc.) and local weather patterns, as well as the interplay with local conditions such as river basin hydrology remains to be settled (cf. National Research Council, 2010). Understanding this relationship requires, among other things, a long-term perspective on precipitation and floods that exceeds the length of available instrumental records.

Records of historic and prehistoric river floods in North America (Hirschboeck, 1987; Knox, 1993, 2000; Ely, 1997), northern Europe (Shorthouse and Arnell, 1999; Phillips *et al*., 2003; Kingston *et al*., 2006a, 2006b, 2009), and central and southern Europe (Benito *et al*., 2003, 2008 Jacobeit *et al*., 2003a; Bouwer *et al*., 2008) are shown to be sensitive to changing atmospheric circulation patterns, underscoring that most instrumental records indeed are too short to properly assess the climate-flood relationship. Jacobeit *et al*. (2003a) show, for instance, that not only is there a historical connection between floods and winter season atmospheric circulation in Central Europe on multi-decadal to centennial time scales, but also that the strength/quality of this relationship has changed during the last 500 years. Periods characterized by frequently reoccurring large floods are associated with meridional flow patterns during the mid-16th and mid-17th century, which is

significantly different from the flood pattern produced by the dominating westerly zonal circulation type.

Ideally, paleoflood records covering several thousands of years can provide valuable information on the long-term variability of flood frequencies and hence address to what extent such alternating patterns can be related to large– to medium scaled atmospheric circulation anomalies and/or local catchment effects. Reconstructed flood records could therefore add insight into how flood frequencies change over longer time scales and also the initial causes of flood frequency and magnitude changes.

Continuous, high-frequent flood records covering large parts of the Holocene (the last 11700 years) are, however, few in number, the most comprehensive being records based on lake sediment cores (e.g. Nesje *et al*., 2001a; Bøe *et al*., 2006; Støren *et al*., 2010), but also speleothems (e.g. Dasgupta *et al*., 2010). Lake records can usually be dated and may potentially store the sedimentary imprint of floods without, at the same time, eroding previous deposits. In sum, this allows for the construction of continuous flood archives spanning thousands of years, which even may overlap with instrumental and historical data. By utilizing two continuous high-resolution lake sediment flood archives from southern Norway, complemented by modern data on wintertime atmospheric circulation anomalies, we address the long-term links between climate change and flood frequency. We show that there are significant changes to the frequency of floods during the mid– to late Holocene which might be linked to atmospheric circulation anomalies different from the NAO.

Study area and methods

The North Atlantic atmospheric circulation patterns have a decisive influence on the climate in Norway, and even small changes in the large-scale winds may result in considerable changes in the spatial distribution of winter precipitation (Hanssen-Bauer and Førland, 2000). Over both inter-annual and decadal timescales, the variations in storminess and winter precipitation over

western Norway are strongly related to changes in the North Atlantic Oscillation (NAO) and the strength and location of the westerly storm track and jet stream (Hurrell *et al*., 2003). Reconstructions of past winter precipitation on the west coast of Norway have therefore been suggested as a possible paleo-indicator for low-frequent variations in the North Atlantic atmospheric circulation patterns (Nesje *et al*., 2000; Bakke *et al*., 2008).

The regional climate in southern Norway is influenced by the topography as well. The Jotunheimen and Rondane mountain areas (>2000 m altitude) create a strong precipitation gradient from southwest to northeast across southern Norway, with mean annual precipitation amounts ranging from more than 4000 mm along the coast to less than 300 mm in the inner (northern) parts of eastern Norway (Fig. 1). The influence of the NAO is decreasing sharply along this transect (Nesje *et al*., 2000; Uvo, 2003; Nordli *et al*., 2005), and eastern Norway receives its main share of precipitation in periods with a more meridional circulation type (Hanssen-Bauer and Førland, 2000; Hanssen-Bauer *et al*., 2009).

Holocene River flood records

The river-flood data analysed in this study are reconstructed from two lakes in southern Norway, Meringsdalsvatnet (MER) in eastern Jotunheimen, and Butjønna (BUTJ) in the northern Østerdalen region (Fig. 1). These are small lakes (0.67 and 0.02 km^2, respectively) in sediment-rich catchments that have proved to successfully record high-frequent flood activity during the Holocene (Drange, 2002; Bøe *et al*., 2006; Støren *et al*., 2010). The geomorphologic characteristics of the two catchments are similar (Table 1), and are thus considered suitable for comparison.

Both lakes are located in alpine mountainous areas where river discharge is dominated by snowmelt (see discussion). The melting season is in May and June in both catchments, with the mean (1971–2009) middle of May snowlines at 820 m (BUTJ), and 900 m (MER) (Fig. 2 and Table 1). The lakes are also located at approximately the same altitude (~650 m). The catchments have an

analogous hypsometric distribution (Fig. 2), although the maximum altitude in the BUTJ catchment is 1272 m (Langfjellet) compared to 1754 m (Heidalsmuen) in the MER catchment. About 12% of the MER catchment area (about 20 km^2) is located above the highest elevation in the BUTJ catchment. The distance between the lakes is approximately 70 km, and the mean annual and monthly temperatures (1968–1990) are similar across the region (Fig. 3). The amount and seasonal distribution of precipitation is also similar, however the MER catchment (station Skåbu) receives slightly more precipitation in all months of the year (Fig. 3).

Both records are previously published, but the sediment core from Butjønna (Bøe *et al*., 2006) was re-measured and re-sampled using exactly the same methodological protocol applied by Støren *et al*. (2010). This study introduces an approach that enables an objective identification of the sedimentary imprint produced by river-floods in lake sediment cores by using the rate of change (RoC) in parameters sensitive to the composition of flood-transported material versus the baseline signal of the lake (Støren *et al*., 2010). In both archives magnetic susceptibility (MS) was measured using a Bartington MS2 point sensor at 2 mm intervals. Records were de-trended to remove the long-term environmental signal, and floods were identified by the positive RoC in MS exceeding 1, 0.75 and 0.5 standard deviation units (σ) (Fig. 4, Table 2). Age-depth relationship in the sediment cores was established by radiometric dating using AMS ^{14}C and $^{210}Pb/^{137}Cs$. All ages are calibrated to calendar years before AD 1950 (cal. a BP), hereafter referred to as years (a) ago. For details on age-depth relationships, see Støren *et al*. (2010) and Bøe *et al*. (2006). The MER core is 502 cm long, covering an age span of 10174 years, giving a mean resolution of 4.0 years/sample, and a minimum resolution of 7.5 years/sample according to the age-depth model. The BUTJ core is 514 cm, covering 9453 years, giving a slightly higher resolution, 3.7 years/sample on average and 6.2 years/sample as a minimum sampling resolution.

Meteorological data

We used monthly precipitation records for the meteorological stations at Skåbu (1969–2009) and Folldal (1959–2006), downloaded from the Norwegian Meteorological Institute's free data server (http://eklima.no). The locations of the stations are indicated in Figure 1. Skåbu is located at 890 m altitude about 4 km south of the MER catchment, and Folldal is located at 710 m altitude, about 7 km west of BUTJ. For the regression against large-scale pressure patterns, we used gridded sea level pressure (SLP) from the NCEP/NCAR reanalysis (Kalnay *et al*., 1996). The NAO index was computed as the first principal component of extended winter (November-March) seasonal mean North Atlantic SLP in the period from 1959 to 2009 inside the region with corners at 20°N, 80°N, 80°W and 40°E. This is the dominant low-frequency pressure pattern in the region – it explains 52% of the variance on the seasonal time scale in the specified period.

Results

Holocene flood records – general trends

Using 1σ, the RoC approach details 92 and 112 flood events in the MER and BUTJ records, respectively. On average, there has been about 1 flood per century during the Holocene (MER=0.9; BUTJ=1.2). The flood activity was generally low during the early and middle Holocene, with means of 0.3 (MER) and 0.7 (BUTJ) floods per century from 7000–5000 years ago. However, the activity increased in the late Holocene, with means of 2.5 (MER) and 2.9 (BUTJ) floods per century from 2300 years ago until present (Fig. 5).

When the identification threshold was lowered to 0.5σ the number of identified floods almost doubles (MER = 180; BUTJ = 198). However, the general Holocene trends remain the same, and the records obtained with these different thresholds are positively correlated: r = 0.90 (MER) and r = 0.75 (BUTJ) ($p < 0.01$) (Table 3). Støren *et al*. (2010) showed that a conservative level of 1σ is sufficient to identify several known historical floods in the MER

core, and to optimize the signal to noise ratio we use this threshold in the following description and discussion.

The BUTJ and MER records show only a weak positive correlation (r = 0.3, $p < 0.01$), and there are distinct differences between them. To examine the relative geographical distribution of floods between the sites, these differences (Δf) were quantified by subtracting the BUTJ record from the MER record (Eq. 1). Due to commensurability of the records and similarities in terms of both variance and the total number of floods recorded, no further standardization of the records was done. The Δf is not significantly affected by the different identification thresholds in the RoC approach (Fig. 5). Correlating Δf obtained using thresholds of 0.5σ and 1σ results in $r = 0.7$ ($p < 0.01$) for the full period. However, prior to 2300 years ago when the flood frequency was low, the correlation coefficient is $r = 0.6$ ($p < 0.01$), compared to $r = 0.8$ ($p < 0.01$) after 2300 years ago, indicating that the Δf is less robust for the early and middle Holocene than over the last 2300 years (Fig. 5). All records are plotted on a centennial scale as the number of events per 100 years. Although the sampling interval allows for a sub-decadal resolution, the age uncertainty of Δf is the product of the combined uncertainties in the radiometric dating and age-depth models used to produce the BUTJ and MER records, which separately have uncertainties around 50-150 years.

$$\Delta f = n_{\mathrm{MER}}{}^{-100a} - n_{\mathrm{BUTJ}}{}^{-100a} \qquad \text{[Eq. 1]}$$

Early Holocene (9700–5600 cal. a BP)

There are no floods recorded in the BUTJ record prior to 6600 years ago. During this part of the core, our approach does not return any positive flood identifications, which suggests quite stable conditions, or possibly that the modern drainage route was not yet established. Thus, the BUTJ record is not regarded as reliable for this period, nor is the Δf record. During the same period (9700–6600 years ago), the MER-record shows moderate, but increased

activity at 8500–8600 years ago (1.0/100a), and 7700–8000 years ago (1.3/100a). Between 6600–5600 years ago, there was increased flood activity in the BUTJ record (1.1/100a), whereas there is only one event in the MER record (0.1/100a), resulting in negative Δf values (Fig. 5).

Mid Holocene (5600–2300 cal. a BP)

From 5600 to 4900 years ago Δf changed sign, due to decreasing activity in the BUTJ record and increasing activity in the MER record. From 4900 up to 2300 years ago there was high activity in BUTJ, peaking 3700–3800 years ago (4/100a). The MER record shows decreased flood activity throughout the period (0.3/100a), resulting in a negative Δf (Fig. 5).

Late Holocene (2300 cal. a BP – present)

A general increase in floods is observed in both records after 2300 years ago. From 2300 to 1200 years ago the MER record was the dominant, peaking 1400–1500 years ago (11/100a), resulting in strong positive values of Δf. Within the last 1200 years the BUTJ record documents a pronounced increase in floods (4.3/100a), which reversed during the last two centuries when the number of floods was reduced (1.5/100a). An abrupt decrease in floods took place between 1200–1000 years ago in the MER record, and persistent low activity from 1000–600 years ago (0.4/100a). From 600 years ago to the present, the number of floods rose again (3.3/100a). Consequently, the Δf thus yields strong negative values from 1000–200 years ago and positive values from 200 years ago until present (Fig. 5).

Winter precipitation and associated atmospheric circulation patterns

In this section, we identify links between atmospheric circulation anomalies and winter precipitation (November–March) at the two meteorological stations that are closest to the two lakes (Skåbu for MER and Folldal for BUTJ, see Fig. 1). The period from 1969 to 2006 is the only period

for which both stations have data, and our analysis is therefore mostly restricted to the inter-annual time scale.

In Figure 6, the results of a linear regression analysis are shown. In the first two panels (Fig. 6a and b), the explained variance (R-squared) and the regression coefficients (β) are shown for univariate models with the standardized winter precipitation of each station as regressors and the SLP as the regressand. The periods used in these models were 1969–2009 for Skåbu, and 1959–2006 for Folldal. The right panel (Fig. 6c) shows the amount of variance explained by a multivariate model where data for both stations in the period from 1969 to 2006 were used. Figure 7 shows the amount of variance explained (contours) and the regression coefficients (arrows) for regression models where the zonal and meridional winds were used as regressands and the precipitations records were used as regressors.

The winter precipitation at Skåbu is associated with regional SLP anomalies over the North Sea (Fig. 6a). The regression model explains up to 40–50% of the inter-annual winter SLP variance. Similar plots for the zonal and meridional wind components show that the precipitation at Skåbu increases in periods with positive anomalies in the southerly component of the flow over Norway (Fig. 7a), as well as stronger than normal westerlies over the British Isles into the northern part of mainland Europe.

Figure 6b shows that the winter precipitation at Folldal is associated with negative SLP anomalies centred over the Bay of Bothnia and positive anomalies centred over the Bay of Biscay. It is similar to the pattern found for Skåbu in that it produces stronger than normal westerlies into northern mainland Europe (Fig. 7b). However, the anomalous meridional wind component over Norway for Folldal is northerly (Fig. 7b). When both stations are used as regressors in a multivariate model, up to 50–60% of the inter-annual SLP fluctuations in a large region centred over the British Isles can be explained (Fig. 6c).

Discussion

Holocene flood frequency

Despite the relative proximity of the two study sites (c. 70 km) (Fig. 1) and the similarities in their catchment conditions, there are marked differences between the reconstructed flood-frequency records (Figs. 4, 5). This raises questions about the underlying mechanisms controlling the flood frequency. What are the relative influences of the local site conditions and the atmospheric circulation?

To conduct a meaningful evaluation of the link between floods and atmospheric circulation patterns, it is important to differentiate between seasons. Although late summer rainstorm events are known to trigger local flood events, the inland parts of Southern Norway are classified as a snowmelt-dominated discharge regime (Gottschalk *et al*., 1979). Snow accumulation causes low runoff during the winter, and high runoff during the snowmelt-season in late spring/early summer when the accumulated water equivalents is released over a short period of time. Historically, the occurrence of large river floods in the region reflects this general discharge pattern. The period 1840-1870 was, for example, dominated by large amounts of snow in the Norwegian mountains, and several major floods were recorded in eastern and southern Norway during this period (Roald, 2002). The discharge and flood frequency are thus, to a large degree dictated by the distribution and amount of solid winter precipitation (Shorthouse and Arnell, 1999; Tveito and Roald, 2005).

Although the amount of snow available at the start of the snowmelt season is assumed to be the most important factor for the occurrence of floods, the course/pattern of melting has historically had an effect on the magnitude of such snowmelt floods. Some of the largest snowmelt floods in southern Norway have occurred when temperatures were low during the spring, and rapidly increased in the summer. Such conditions make snowmelt at low and high altitudes possible at the same time and may potentially lead to large floods if the accumulated snow magazine is sufficient, such as in the case of the major "Stor-Ofsen" event in 1789 and "Vesle-Ofsen" in 1995 (Østmoe 1985; Eikenæs

et al., 2000).

As the methodology used to identify floods does not differentiate flood types, the potential impact of summer rainstorm-floods must, however, be considered as noise in the analysis of links between wintertime atmospheric circulation and flood frequency.

At present the snow-melting season in the study areas is in May and June. With changing temperatures and land uplift during the Holocene, this has fluctuated accordingly. We employ a simple model based on the following assumptions: 1°C warmer summer conditions during the Holocene Thermal Maximum (HTM) (about 6000 years ago); 1°C colder summers during the Neoglacial (about 2000 years ago) (Seppä *et al*., 2009); a lapse rate of 0.6°C per 100 m (Green and Harding, 1980); and a land uplift of about 45 m during the last 6000 years (Kjemperud, 1981; Lie and Sandvold, 1997). The model indicates that both catchments have been covered with snow for more than four months during the winter season throughout the Holocene, and the snowmelt potential is probably sufficient in both catchments to produce continuous records of snowmelt floods. The length of the snow season and the size of the snow-covered area have, however, changed during the Holocene, possibly affecting the mechanisms that trigger snowmelt floods (Table 3 and Fig. 2). Also assuming a nonlinear increase in precipitation towards higher altitudes (e.g. Laumann and Reeh, 1993), the snowmelt potential may have increased significantly during the Holocene. Combined with a general increase in reconstructed winter precipitation (Nesje *et al*., 2001b; Bjune *et al*., 2005) over the last 6000 years, this may explain the general increasing trend – from a low flood frequency during the HTM to a high frequency during the Neoglacial – as observed in both catchments. The major increase in flood frequency over the last two millennia is most likely a response to a general increase in winter precipitation over Southern Norway. Similar increases have been recorded in several glacier and winter precipitation reconstructions from southern Norway (see. e.g. Bakke *et al*., 2008; Nesje, 2009). Foraminifera-based North Atlantic SST reconstructions, interpreted as a annual mean or winter signal (Jansen *et*

al., 2008) also indicate a rapid shift towards warmer conditions at this time (eg. Andersson *et al*., 2010). We therefore regard the winter season signal in the flood records to be stronger during this period than during the early and middle Holocene, when sporadic summer rainstorms may have influenced the records to a larger degree.

Following the above argumentation, the flood frequency in southern Norway is influenced by mechanisms on a wide range of timescales, from tectonic to seasonal. However, due to the proximity of the two catchments studied here, changing catchment conditions due to land uplift, temperature changes and associated changes in e.g. vegetation cover, have probably affected both areas in similar ways during the Holocene. We therefore regard the flood records as truly comparable with similar catchment conditions and dominant flood-triggering processes. Their differences, expressed by Δf, are suggested to reflect site-specific changes related to external multi-decadal to centennial-scale mechanisms that control the snowmelt potential in the catchments.

Relating atmospheric circulation anomalies to flood activity

The external factor that is most likely controlling Δf involves the relative differences in the amount of solid winter precipitation caused by shifts in the atmospheric circulation transporting moist air from the North Atlantic over Southern Norway. Previous studies of observational/historical (Hurrell, 1995; Luterbacher *et al*., 2002) and proxy data (Appenzeller *et al*., 1998; Cook *et al*., 2002; Meeker and Mayewski, 2002; Rimbu *et al*., 2003; Trouet *et al*., 2009) indicate that variability in North Atlantic atmospheric circulation, in particular the NAO, is detectable on multi-year time scales from inter-annual to millennial. Although the NAO explains about half of the SLP variance in the North Atlantic region on the inter-seasonal time scale in the recent decades, there are also important lower-order principal components of SLP in this region, such as the ones that are often referred to as the East Atlantic Pattern, the Scandinavian Pattern and the East Atlantic/Western Russia Pattern (eg.

Barnston and Livezey, 1987; Hurrell *et al*., 2003; Cassou, 2008). Jacobeit et al. (2003b), using the dataset of Luterbacher et al. (2002), show that the dominance of NAO has changed over time. During a period in the middle 19th century, for example, a meridional flow pattern seams to have been the dominant pattern of the North Atlantic atmospheric circulation.

For our regression analysis of the winter precipitation and large-scale pressure patterns, only 41 and 48 years of instrumental data were available from the study areas. It must therefore be emphasized that this is not a rigid analysis of variability on the multi-year time scale. However, considering the discussion above, it is not unlikely that centennial-scale variations in atmospheric circulation and associated winter precipitation have influenced variations the flood frequency in Southern Norway. We therefore employ the observations during the instrumental period as a possible modern analogue for prevailing anomalies in the Holocene atmospheric circulation.

During the instrumental period, we see marked differences in the amount and distribution of winter precipitation between the study areas. Figure 6 shows that the largest amounts of precipitation close to the MER catchment (station Skåbu) are recorded in periods with low anomalies over the northern North Sea and anomalous southerly winds, whereas high precipitation in the BUTJ catchment (station Folldal) occurs in periods with anomalous north-westerly flow, lower-than normal pressure over the Bay of Bothnia and high-pressure anomalies over the Bay of Biscay.

As mentioned earlier, the winter precipitation at many locations in Norway is strongly correlated with the NAO index, which is typically associated with increased frequencies and strengths of the moist southwesterlies over large regions of the northern and northeastern Atlantic in its positive phase. The amount of SLP variance on the inter-seasonal time scale explained by winter precipitation at Skåbu and Folldal is relatively high over a region that covers much of the North Sea (Fig. 6c). This pattern is distinctly different from the loading pattern of the NAO (Fig. 8a). Figure 8b shows the inter-annual fluctuations of the NAO index (blue curve) and the winter mean precipitation at

Skåbu (gray curve) and Folldal (black curve). The correlation between the stations and the NAO index after different levels of smoothing have been applied are shown in Figure 8c; the y-axis indicates the number of years that were used to compute running averages and the x-axis shows the correlation coefficients on the different time scales. In the study period there is little correlation between the NAO index and the winter precipitation at Skåbu and Folldal, even when we used running averages over several years (which reduces number of degrees of freedom and tends to lead to higher correlation coefficients when the data are correlated in the first place).

Applying the period of observational data as an analogue for past and future variability, the above analysis has two important implications: 1) The NAO cannot be used to reconstruct past and future floods in our study regions; and 2) When reconstructing past atmospheric circulations, our flood records (Fig. 5) have the potential to yield important information about pressure fluctuations in regions that are not influenced by the NAO (Fig. 6).

From 6600 to 2300 the flood frequencies in both records and the variability of Δf are, in general, low. The authority of the Δf to indicate shifts in atmospheric circulation over this period is therefore limited. However, using an identification level of 0.5σ, increasing the number of events, the long-term tendencies over the period are not changed (Fig. 5), indicating some degree of reliability. Negative Δf values between 6600 and 5600 and 4900–2300 years ago may thus indicate circulation anomalies similar to that associated with increased activity in the BUTJ catchment (Fig. 6b and 7b). About 2300 years ago the variability and number of floods began to increase, and the strong positive Δf at 2300-1200 years ago (Fig. 5) is associated with a dominant southerly circulation component at the time (Fig. 6a and 7a), weakening from 1500 to about 600 years ago when Δf was decreasing. This coincides with increased strength of the southwesterlies (Bakke *et al*., 2008), peaking around 1800 years ago and decreasing towards present, and reduced winter precipitation on southwest-coast glaciers (Fig. 1) at about 1000-500 years ago

(Nesje, 2009). Meeker and Mayewski (2002), found that winter season Siberian High, Icelandic low and Azores High shifted from weak to strong entering the "Little Ice Age" (LIA) (c. AD 1400), implying a more intense winter circulation over the North Atlantic during the LIA.

Conclusion

By analyzing two continuous, high-resolution sediment records from southern Norway, as well as winter precipitation and associated atmospheric circulation anomalies in the two regions we draw the following conclusions:

- The frequency of extreme flood events in southern Norway has changed significantly during the Holocene. The period after about 2300 years ago stands out with the shortest flood recurrence interval over the Holocene. During this period, the mean flood frequency was 2-3 times the Holocene mean, which is approximately 1 flood per century. During the early and middle Holocene the flood frequency was low, around one half of the Holocene mean.
- The two paleoflood records reveal subtle differences over a short distance, producing a pattern that alternates on multi-decadal to centennial time scales. Our results indicate that these changing frequencies in flood frequency cannot be explained by local conditions associated with the respective catchments of the two lakes. Rather, long-term trends in the flood activity appear to reflect variations of solid winter precipitation and related spring/summer snowmelt.
- Using available modern meteorological data, we document that atmospheric circulation anomalies, distinctly different from the North Atlantic Oscillation (NAO), have some potential in explaining the two different flood patterns, and that the NAO cannot be used to reconstruct past and future floods in our study regions. During the instrumental period the two regions receive winter precipitation during northerly (BUTJ) and southerly (MER) circulation anomalies.
- Employing the instrumental data as a modern analogue for Holocene

changes, the flood records from southern Norway are indicative of centennial-scale shifts in regional weather patterns, and can potentially yield information about past pressure fluctuations in regions that are not influenced by the North Atlantic Oscillation (NAO). Major shifts in river flood frequency are recorded at about 2300, 1200, and 200 years ago.

Acknowledgement

We offer our sincere thanks to Dr. Anne-Grete Bøe and Prof. Svein Olaf Dahl at the Department of Geography, University of Bergen, for making the cores from Butjønna available for further analysis. Prof. Atle Nesje provided valuable comments on the manuscript. Laboratory analysis was performed at Prof. Reidar Løvlie's Paleomagnetic Laboratory (University of Bergen, Department of Earth Science). This is publication no. XX from the Bjerknes Centre for Climate Research.

References

Andersson C, Pausata FSR, Jansen E, Risebrobakken B, Telford RJ (2010) Holocene trends in the foraminifer record from the Norwegian Sea and the North Atlantic Ocean. Climate of the Past 6:179–193

Allen MR, Ingram WJ (2002) Constrains on future changes in climate and the hydrological cycle. Nature 419:224-232

Appenzeller C, Stocker TF, Anklin M (1998) North Atlantic Oscillation dynamics recorded in Greenland ice cores. Science 282 (5388):446-449

Bakke J, Lie Ø, Dahl SO, Nesje A, Bjune AE (2008) Strength and spatial patterns of the Holocene wintertime westerlies in the NE Atlantic region. Global and Planetary Change 60:28-41

Barnston AG, Livezey RE (1987) Classification, seasonality and persistence of low-frequency atmospheric circulation patterns. Monthly Weather Review 115:1086-1126

Benito G, Sopena A, Sánchez-Moya Y, Machado M, Pérez-Gonzáles A (2003) Paleflood record of the Tangus River (central Spain) during the Late Pleistosene and Holocene. Quaternary Science Reviews 22:1737-1756

Benito G, Thorndycraft VR, Rico M, Sanchez-Moya Y, Sopena A (2008) Palaeoflood and floodplain records from Spain: Evidence for long-term climate variability and environmental changes. Geomorphology 101(1-2):68-77

Bjune AE, Bakke J, Nesje A, Birks HJB (2005) Holocene mean July temperature and winter precipitation in western Norway inferred from palynological and glaciological lake-sediment proxies. The Holocene 15 (2):177-189

Bouwer LM, Vermaat, JE., Aerts, JCJH (2008) Regional sensitivities of mean and peak river discharge to climate variability in Europe. Journal of Geophysical Research 113

Bøe A-G, Dahl SO, Lie Ø, Nesje A (2006) Holocene river foods in the upper Glomma catchment, southern Norway: a high-resolution multiproxy record from lacustrine sediments. The Holocene 16 (3):445-455

Cassou C (2008) Intraseasonal interaction between the Madden-Julian Oscillation and the North Atlantic Oscillation. Nature 455:523-527

Cook ER, D´Arrigo RD, Mann M (2002) A well-verified, multiproxy reconstruction of the winter North Atlantic Oscillation index since A.D. 1400. Journal of Climate 15:1754-1764

Dahl SO, Nesje A (1996) A new approach to calculating Holocene winter precipitation by combining glacier equlibrium-line altitudes and pine-tree limits: a case study from Hardangerjøkulen, central southern Norway. The Holocene 6:381-398

Dasgupta S, Saar MO, Edwards RL, Shen C-C, Cheng H, Alexander Jr EC (2010) Three thousand years of extreme rainfall events recorded in stalagmites from Spring Valley Caverns, Minnesota. Earth and Planetary Science Letters:doi:10.1016/j.epsl.2010.1009.1032

Drange EM (2002) Et paleohydrologisk studie av Sagbekken, Hedmark fylke: En rekonstruksjon av Sagbekkens flomhistorie gjennom holosen (in Norwegian). Master thesis, University of Bergen,

Eikenæs O, Njøs A, Østdahl T, Taugbøl T (2000) Flommen kommer... Sluttrapport fra HYDRA -et forskningsprogram om flom. Norwegian Water Resources and Energy Directorate (NVE) (in Norwegian), Oslo

Ely L (1997) Responce of extreme floods in the sothwestern United States to climatic variations in the late Holocene. Geomorphology 19:175-201

Gottschalk L, Jensen JL, Lundquist D, Solantie R, Tollan A (1979) Hydrologic Regions in the Nordic Countries. Nordic Hydrology 10:273-286

Green FHW, Harding RJ (1980) The altitudinal gradients of air temperature in southern Norway. Geografiska Annaler 62 (1):29-36

Hanssen-Bauer I, Drange H, Førland EJ, Roald LA, Børsheim KY, Hisdal H, Lawrence D, Nesje A, Sandven S, Sorteberg A, Sundby S, Vasskog K, Ådlandsvik B (2009) Klima i Norge 2100. Bakgrunnsmateriale til NOU Klimatilplassing. Norsk klimasenter Oslo (in Norwegian)

Hanssen-Bauer I, Førland E (2000) Temperature and precipitation variations in Norway 1900-1994 and their links to atmospheric circulation. International Journal of Climatology 20:1693-1708

Hirschboeck KK (1987) Catastrophic flooding and atmospheric circulation patterns. In: Mayer L, Nash D (eds) Catastrophic Flooding. Allen and Unwin, Boston, pp 23–56.

http://eklima.no, Norwegian Meteorological Institute's web pages: Accessed September 2010

http://senorge.no, Accessed September 2010

Hurrell JW (1995) Decadal trends in the North-Atlantic Oscillation - regional temperatures and precipitation. Science 269 (5224):676-679

Hurrell JW, Kushnir Y, Ottersen G, Visbeck M (2003) An Overview of the North Atlantic Oscillation. In: Hurrell JW, Kushnir Y, Ottersen G, Visbeck M (eds) The North Atlantic Oscillation: Climatic significance and environmental impact, Geophysical Monograph 134. American Geophysical Union, pp 1-35

IPCC (2007) Climate Change 2007, Fourth Assessment Report of the Intergovernmental Panel on Climate Change.

Jacobeit J, Glaser R, Luterbacher J, Wanner H (2003a) Links between flood events in central Europe since AD 1500 and large-scale atmospheric circulation modes. Geophysical Research Letters 30 (4)

Jacobeit J, Wanner H, Luterbacher J, Beck C, Philipp A, Sturm K (2003b) Atmospheric circulation variability in the North-Atlantic-European area since the mid-seventeenth century. Climate Dynamics 20:341-352

Jansen E, Andersson C, Moros M, Nisancioglu KH, Nyland BF, Telford RJ (2008) The early to mid-Holocene thermal optimum in the North Atlantic In: Battarbee RW, Binney HA (eds) Natural Climate Variability and Global Warming – A Holocene Perspective. Wiley-Blackwell, Chichester, pp 123–137

Kalnay E, Kanamitsu M, Kistler R, Collins W, Deaven D, Gandin L, Iredell M, Saha S, White G, Woollen J, Zhu Y, Leetmaa A, Reynolds R, Chelliah M, Ebisuzaki W, W.Higgins, Janowiak J, Mo KC, Ropelewski C, Wang J, Jenne R, Joseph D (1996) The NCEP/NCAR 40-Year reanalysis project. Bulletin of the American Meteorological Society 77:437-470

Kingston DG, Hannah DM, Lawler DM, McGregor GR (2009) Climate-river flow relationships across montane and lowland environments in northern Europe. Hydrological Processes 23:985-996

Kingston DG, Lawler DM, McGregor GR (2006a) Linkages between atmospheric circulation, climate and streamflow in the northern North Atlantic: research prospects. Progress in Physical Geography 30 (2):143-174

Kingston DG, McGregor GR, Hannah DM, Lawler DM (2006b) River flow teleconnections across the northern North Atlantic region. Geophysical Research Letters 33

Kjemperud A (1981) A shoreline displacement investegation from Frosta in Trondhjemsfjorden, Nord-Trøndelag, Norway. Norsk Geografisk Tidsskrift 61:1-15

Knox JC (1993) Large increases in flood magnitude in response to modest changes in climate. Nature 361 (6411):430-432

Knox JC (2000) Sensitivity of modern and Holocene floods to climate change. Quarternary Science Reviews 19:439-457

Laumann T, Reeh N (1993) Sensitivity to climate-change of the mass-balance of glaciers in southern Norway. Journal of Glaciology 39 (133):656-665

Lie Ø, Sandvold S (1997) Late Weichselian - Holocene glacier and climate variations in eastern Jotunheimen, south-central Norway. Cand.polit. Thesis, University of Bergen,

Luterbacher J, Xoplaki E, Dietrich D, Jones P, Davies T, Portis D, Gonzalez-Rouco J, von Storch H, Gyalistras D, Casty C, Wanner H (2002) Extending North Atlantic Oscillation reconstructions back to 1500. Atmospheric Science Letters doi:10.1006/asle.2001.0044.

McCarthy J, Canziani O, Leary N, Dokken D, White K (2001) Climate Change 2001: Impacts, Adaptations and Vulnerability. University Press, Cambridge

Meeker LD, Mayewski PA (2002) A 1400-year high-resolution record of atmospheric circulation over the North Atlantic and Asia. The Holocene 12 (3):257–266

National Research Council (2010) Climate Stabilization Targets: Emissions, concentrations, and impacts over decades to millennia, Committee on Stabilization Targets for Atmospheric Greenhouse Gas Concentrations; National academies press, Wachington D.C. (2010).

Nesje A (2009) Latest Pleistocene and Holocene alpine glacier fluctuations in Scandinavia Quaternary Science Reviews 28 (21-22):2119-2136

Nesje A, Dahl SO, Lie O (2000) Is the North Atlantic Oscillation reflected in Scandinavian glacier mass balance records? Journal of quaternary science 15 (6):587-601

Nesje A, Dahl SO, Matthews JA, Berrisford MS (2001a) A 4500- year history of river floods from eastern Norway: high resolution evidence from lacustrine sediments in Atnsjøern. Journal of Paleolimnology 25:329-342

Nesje A, Matthews JA, Dahl SO, Berrisford MS, Andersson C (2001b) Holocene glacier fluctuations of flatebreen and winter-precipitation changes in the Jostedalsbreen region, western Norway, based on glaciolacustrine sediment records. The Holocene 11(3):267–280

Nordli Ø, Lie Ø, Nesje A, Benestad R (2005) Glacier mass balance in southern Norway modelled by circulation indices and spring-summer temperatures AD 1781-2000. Geografiska Annaler 87A:431-445

Phillips ID, McGregor GR, Wilson CJ, Bower D, Hannah DM (2003) Regional climate and atmospheric circulation controls on the discharge of two British rivers, 1974–97. Theoretical and Applied Climatology 76:141-164

Rimbu N, Lohmann G, Kim JH, Arz HW, Schneider R (2003) Arctic/North Atlantic Oscillation signature in Holocene sea surface temperature trends as obtained from alkenone data, . Geophysical Research Letters 30

Roald, LA (2002) The large flood of 1860 in Norway, in: Snorrason, A., Finnsdottir, HP., Moss, ME. (Eds) The Extremes of the Extreme: Extraordinary Floods

(Proceedings of a symposium held at Reykjavik, Iceland July 2000) IAHS Publ. no. 271

Seppä H, Bjune AE, Telford RJ, Birks HJB, Veski S (2009) Last nine-thousand years of temperature variability in Northern Europe. Climate of the Past Discussions 5:1521-1552

Shorthouse C, Arnell N (1999) The effects of climatic variability on spatial characteristics of european river flows. Phys. Chem. Earth (B) 24 (1-2):7-13

Solomon S, Plattner GK, Knutti R, Friedlingstein P (2009) Irreversible climate change due to carbon dioxide emissions. PNAS 106(6):1704-1709

Støren EN, Dahl SO, Nesje A, Paasche Ø (2010) Identifying the sedimentary imprint of high-frequency Holocene river floods in lake sediments: Development and application of a new method. Quaternary Science Reviews 29:3021-3033

Trouet V, Esper J, Graham NE, Baker A, Scourse JD, Frank1 DC (2009) Persistent positive North Atlantic Oscillation mode dominated the Medieval Climate Anomaly. Science 324:78-80

Tveito OE, Roald LA (2005) Relations between long-term variations in seasonal runoff and large scale atmospheric circulation patterns. met.no report vol no. 7. Norwegian Meteorological Institute,

Uvo C (2003) Analysis and regionalization of Northern European winter precipitation based on its relationship with the North Atlantic Oscillation. International Journal of Climatology 23:1185-1194

Østmoe A (1985) Stor-ofsen 1789 (in Norwegian). Oversiktsregisteret, Ski

Tables

Table 1: Key characteristics for Meringsdalsvatnet (MER) and Butjønna (BUTJ) catchments. Climate data are from meteorological stations Folldal (9110) (710 m) and Skåbu (13670) (890 m) (http://eklima.no). Snow data collected from http://senorge.no.

Catchment characteristics	MER	BUTJ
Catchment area (km^2)	171	22
Lake area (km^2)	0.67	0.02
Lake area / catchment area	0.004	0.001
Lake altitude (m)	634	667
Mean altitude (m)	990	960
Maximum altitude (m)	1754	1272
Mean (1971-2009) May snow line altitude (m)	900	820
Mean (1968-1990) annual precip. (mm)	540 (Skåbu)	365 (Folldal)
Mean (1968-1990) annual temp. (°C)	0.5 (Skåbu)	0.7 (Folldal)

Table 2: Pearson correlation coefficients (r) for BUTJ and MER records where floods are identified using RoC exceeding 1, 0.75 and 0.5 standard deviation units (σ). All the correlation coefficients are significant at the 0.01 level.

	BUTJ 1σ	BUTJ 0.75σ	BUTJ 0.5σ	MER 1σ	MER 0.75σ	MER 0.5σ
BUTJ 1σ (n floods = 112)	1					
BUTJ 0.75σ (n floods = 140)	0.88	1				
BUTJ 0.5σ (n floods = 198)	0.75	0.88	1			
MER 1σ (n floods = 92)	0.31	0.36	0.48	1		
MER 0.75σ (n floods = 120)	0.37	0.42	0.55	0.95	1	
MER 0.5σ (n floods = 180)	0.38	0.45	0.61	0.90	0.94	1

Table 3: Scenarios for changes in Holocene snow cover in the two catchments. Present conditions are a mean of data from 1971-2009 (http://senorge.no). Holocene Thermal Maximum (HTM) and Neoglacial (Neo) conditions are estimated using present conditions plus and minus 1 °C respectively, and adjusted for land uplift using the curve by Kjemperud *et al*. (1981) modified by Lie and Sandvold (1997).

	Present	Neoglacial (Neo)	HTM	Neo-HTM
MER				
100% snow cover (months)	5.3	6.1	4.4	1.7
50 % snow cover (months)	6.6	7.3	5.7	1.6
> 0 % snow cover (months)	10.6	12	9.3	2.7
0 % snow cover (months)	1.4	0	2.7	-2.7
% snow cover in mid May	67 %	90 %	31 %	59 %
Mid May snowline altitude (m)	900	775	1110	-335
BUTJ				
100% snow cover (months)	5.4	6.4	4.2	2.2
50 % snow cover (months)	7.1	8.0	6.0	2.0
> 0 % snow cover (months)	8.8	10.2	7.9	2.3
0 % snow cover (months)	3.2	1.8	4.1	-2.3
% snow cover in mid May	92 %	100 %	46 %	54 %
Mid May snowline altitude (m)	820	634	967	-333

Figures

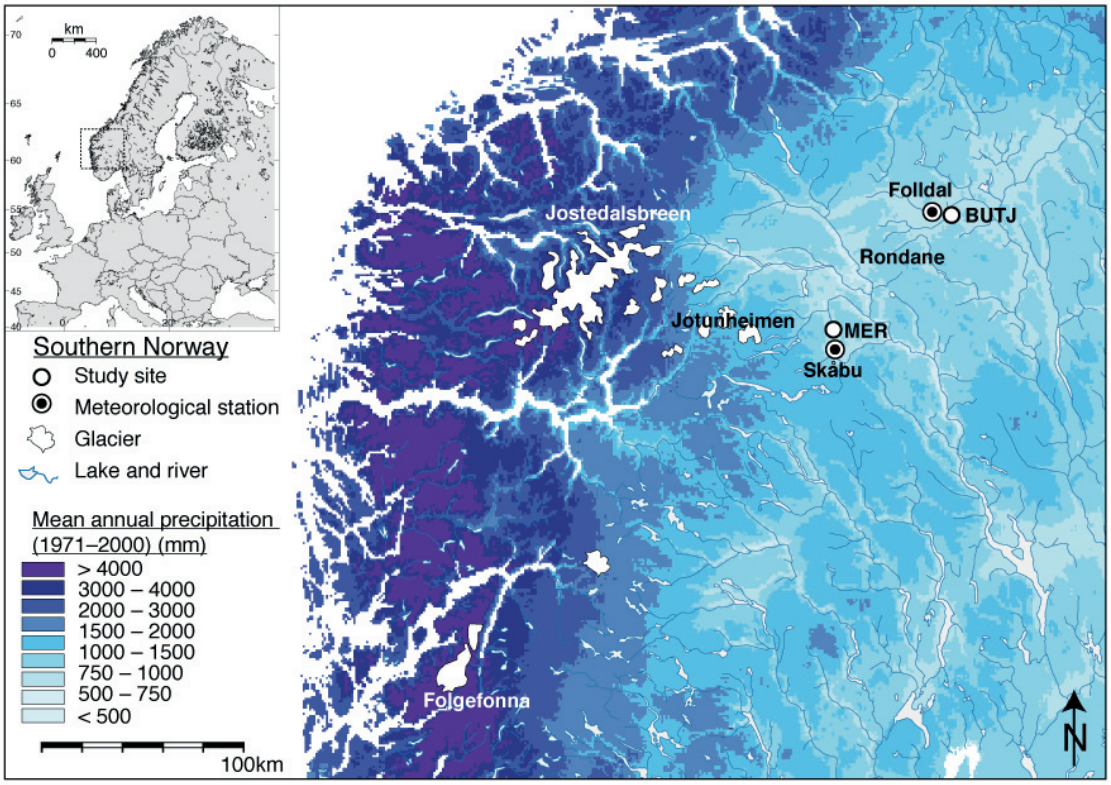

Fig. 1: Map of southern Norway with colours indicating mean annual precipitation (1971-2000) (http://senorge.no). Location of flood records Meringsdalsvatnet (MER) and Butjønna (BUTJ), and location of meteorological stations Skåbu (890 m) and Folldal (710 m) are indicated.

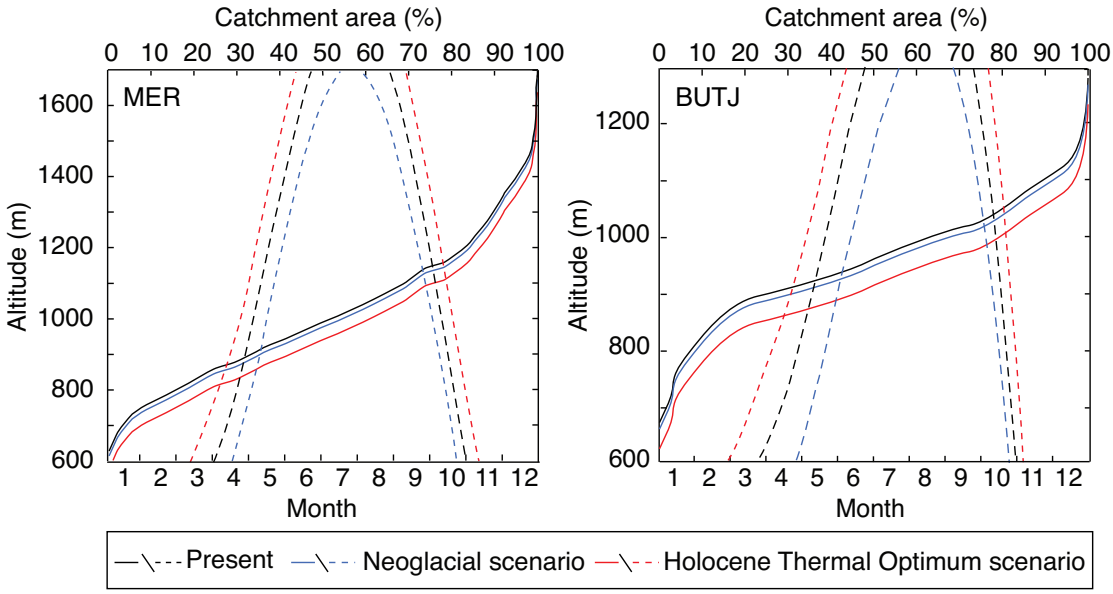

Fig. 2: Hypsometric curve (solid) and mean monthly altitude of the snowline (dotted) in the MER and BUTJ catchments. Scenarios for the Neoglacial (–10m) and Holocene thermal maximum (–45m) hypsometry are calculated using a land uplift curve by Kjemperud *et al*. (1981) adjusted by Lie and Sandvold (1997). Neoglacial (–1°C) and thermal maximum (+1°C) snowlines are calculated using an adiabatic lapse rate of 0.6 100^{-1} m. Snow data are collected from http://senorge.no.

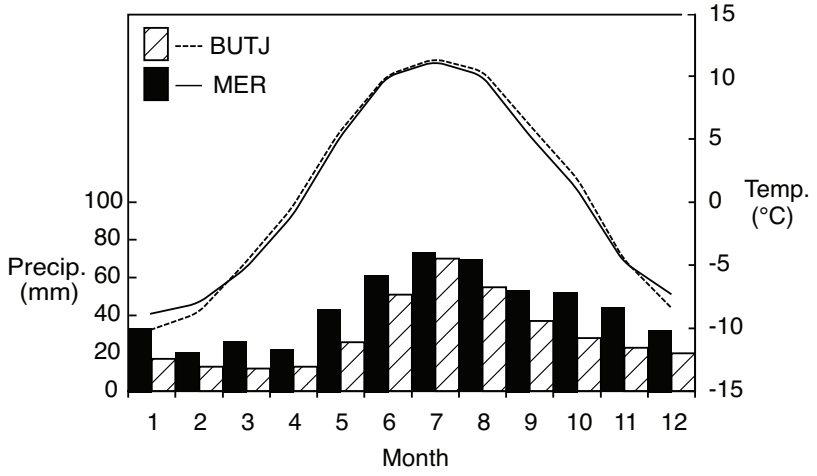

Fig. 3: Climatogram of meteorological data from Skåbu (4 km from MER) and Folldal (7 km from BUTJ). Data from the Norwegian Meteorological Institute (http://eklima.no).

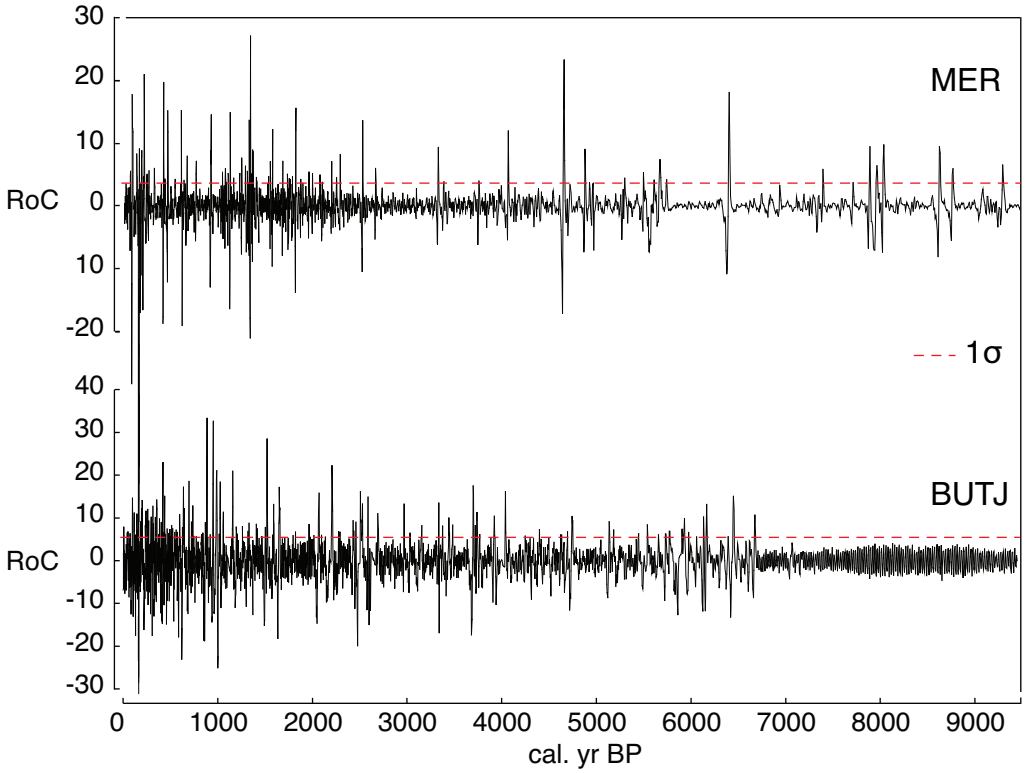

Fig. 4: Rate of change (RoC) in magnetic susceptibility (MS) calculated for MER (upper panel) and BUTJ (lower panel). The one standard deviation (1σ) level (dotted red line) is indicated as threshold for positive identification of floods. Note the low variability in the BUTJ record before 6600 years ago, witch possibly indicates the modern drainage route was not yet established.

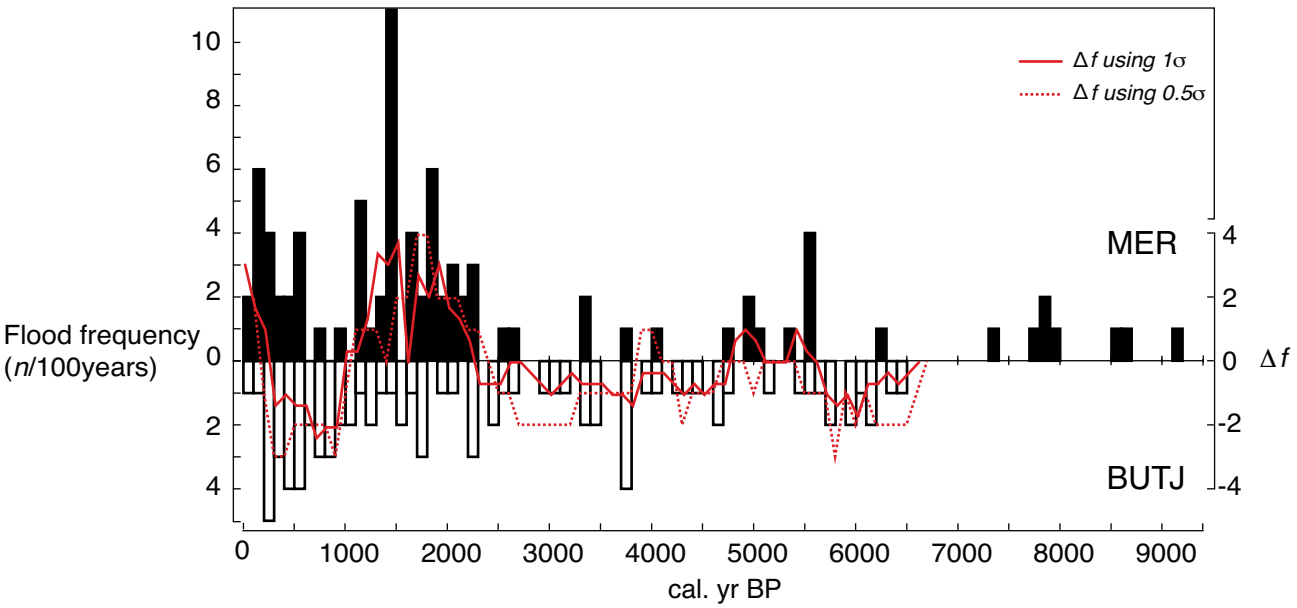

Fig. 5: Flood frequency for MER (black) and BUTJ (white) catchments. The Δf (MER – BUTJ) is calculated using identification thresholds of 1σ (full red line) and 0.5σ (dotted red line) plotted as three hundred year running averages.

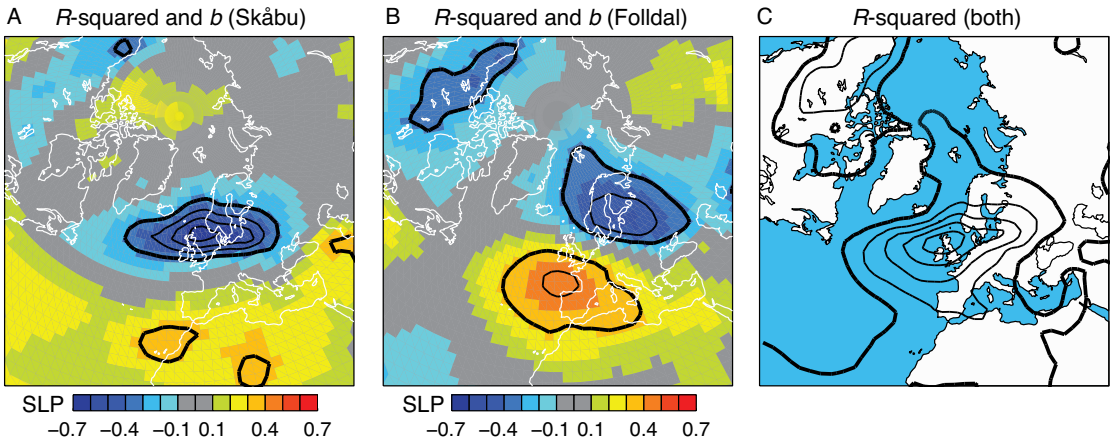

Fig. 6: Linear regression models with winter precipitation as regressors and SLP as the regressand. All the parameters were standardised. The black contours show the R^2-values of the models (i.e. the amount of SLP variance explained) for the stations at Skåbu (**a**) and Folldal (**b**) and both stations (**c**). The unit is standard deviation units, the contour interval is 0.1 and the contours start with the bold curve for $R^2 = 0.1$. The colours in the left two panels show the regression coefficients β, also in standard deviation units.

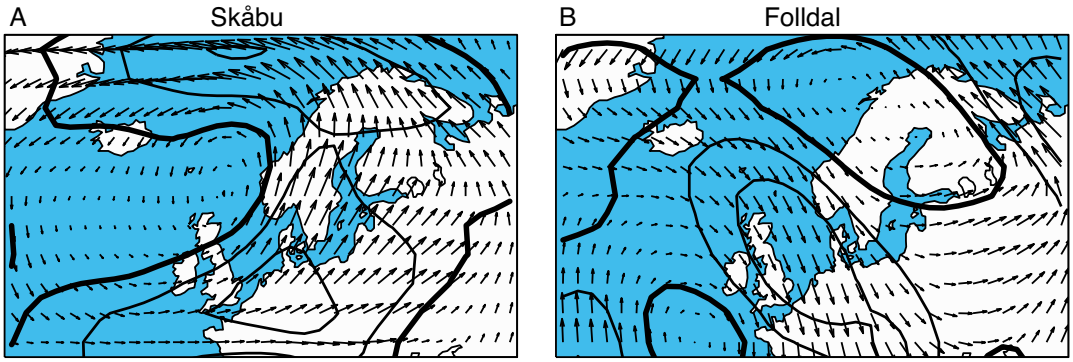

Fig. 7: Linear regression models with winter precipitation as regressors and zonal and meridional winds as the regressands. The regression coefficients are plotted as wind vectors, and the longest vector corresponds to a regression coefficient vector with length 0.5. The black contours show the R^2-values of the models for the stations at Skåbu (a) and Folldal (b). Contour interval is 0.1 for R^2 and the contours start with a bold curve for $R^2 = 0.1$. The unit is standard deviation units.

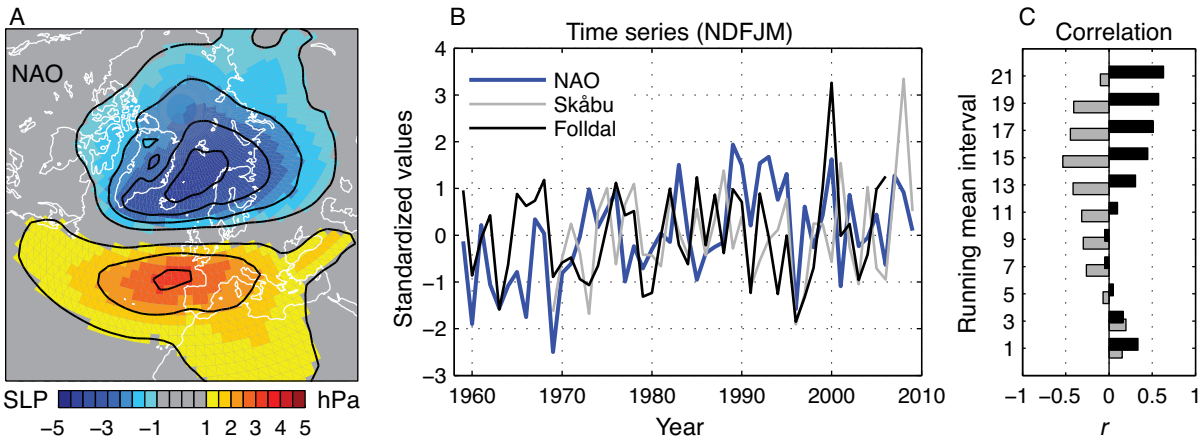

Fig. 8: (**a**) The spatial loading pattern of the NAO as SLP regressed on the first principal component of winter mean SLP in the North Atlantic sector with corners at 90°W, 40°E, 20°N and 80°N (the NAO index). (**b**) The standardized time series for the NAO index and winter precipitation at the stations. (**c**) The correlation coefficients between the NAO index and the winter mean precipitation at the stations after the application of running mean filters with widths corresponding to the values at the y-axis (1 means no smoothing, 3 means 3-year running means and so on).